



Site M0105¹

Contents

- 1 Operations
- 2 Lithostratigraphy
- 4 Physical properties
- 5 Geochemistry
- 7 Paleomagnetism
- 8 Geochronology
- 8 References

Keywords

International Ocean Discovery Program, IODP, Expedition 389, *MMA Valour*, Hawaiian Drowned Reefs, Earth climate system, Earth system feedbacks, Earth history tipping points, Site M0105, coral reef, volcanics, sea level, paleoclimate, central Pacific, reef health, Hawaiian geology, basalt, lava, carbonates, Hilo

Core descriptions

Supplementary material

References (RIS)

MS 389-112

Published 26 February 2025

Funded by ECORD, JAMSTEC, and NSF OCE1326927

J.M. Webster, A.C. Ravelo, H.L.J. Grant, M. Rydzy, M. Stewart, N. Allison, R. Asami, B. Boston, J.C. Braga, L. Brenner, X. Chen, P. Chutcharavan, A. Dutton, T. Felis, N. Fukuyo, E. Gischler, S. Greve, A. Hagen, Y. Hamon, E. Hathorne, M. Humblet, S. Jorry, P. Khanna, E. Le Ber, H. McGregor, R. Mortlock, T. Nohl, D. Potts, A. Prohaska, N. Prouty, W. Renema, K.H. Rubin, H. Westphal, and Y. Yokoyama²

¹Webster, J.M., Ravelo, A.C., Grant, H.L.J., Rydzy, M., Stewart, M., Allison, N., Asami, R., Boston, B., Braga, J.C., Brenner, L., Chen, X., Chutcharavan, P., Dutton, A., Felis, T., Fukuyo, N., Gischler, E., Greve, S., Hagen, A., Hamon, Y., Hathorne, E., Humblet, M., Jorry, S., Khanna, P., Le Ber, E., McGregor, H., Mortlock, R., Nohl, T., Potts, D., Prohaska, A., Prouty, N., Renema, W., Rubin, K.H., Westphal, H., and Yokoyama, Y., 2025. Site M0105. In Webster, J.M., Ravelo, A.C., Grant, H.L.J., and the Expedition 389 Scientists, Hawaiian Drowned Reefs. Proceedings of the International Ocean Discovery Program, 389: College Station, TX (International Ocean Discovery Program).
<https://doi.org/10.14379/iodp.proc.389.112.2025>

²Expedition 389 Scientists' affiliations.

1. Operations

The multipurpose vessel *MMA Valour* was used as the drilling platform throughout Expedition 389. At all Expedition 389 sites, dynamic positioning was used to provide accurate positions throughout operations and water depth was established using a Sound Velocity Profiler (SVP) placed on the top of the PROD5 drilling system. For more detail on acquisition methods, see **Introduction** in the Expedition 389 methods chapter (Webster et al., 2025a).

Summary operational information for Site M0105 is provided in Table **T1**. All times stated are in Hawaiian Standard Time (HST).

1.1. Hole M0105A

The *MMA Valour* arrived on location at 0555 h on 16 October 2023. PROD5 was deployed at 0950 h at a water depth of 339.5 m. Rotary coring and casing in Hole M0105A began at 0959 h and continued to 26.08 meters below seafloor (mbsf) at 0649 h on 17 October. The borehole was terminated to allow recovery of core barrels and casing and transit to port to address a medical issue with a drilling contractor. PROD5 was recovered to deck by 0805 h, when on-deck operations commenced and core barrels were extracted for curation. Transit to the port of Hilo began at 0805 h on 17 October, and the vessel came alongside at 1036 h to allow the contractor to disembark. The *MMA Valour* departed port and the working area at 1125 h on 17 October in a southerly direction toward Site M0106 due to a forecast of heavy seas in the Hilo area.

A total of 14 cores were recovered from Hole M0105A from a total of 26.08 m of rotary coring. The recovered length of core was 7.63 m (29.26%).

Table T1. Hole summary, Site M0105. R = rotary coring mode. LAT = Lowest Astronomical Tide. [Download table in CSV format.](#)

Hole	Water depth (mbsf)	Date started (2023)	Date finished (2023)	Latitude	Longitude	Coring method	Total drilled depth (m)	Recovered length (m)	Core recovery (%)	Cores (N)	Notes
389-M0105A	339.5	16 Oct	17 Oct	19.867494°	-154.972719°	R	26.08	7.63	29	14	LAT water depth: 339.1. Borehole terminated due to port call.

2. Lithostratigraphy

Site M0105 was drilled at 339.5 meters below sea level (mbsl) to 26.14 mbsf in the Hilo region with very low recovery of nonvolcanic lithologies. Hole M0105A is divided into four main intervals:

- Interval 1 (0.00–0.32 mbsf) is composed of rhodoliths in a dark gray unconsolidated bioterrital and volcanoclastic sandy matrix. Because of poor recovery, the base of this interval is unknown.
- Interval 2 (7.43–7.69 mbsf) is dominated by algal boundstone. Because of poor recovery, the vertical extent and the boundaries of this interval are unknown.
- Interval 3 (12.95–15.46 mbsf) is dominated by a fragmented coralg al boundstone (predominantly columnar and robust branching *Porites*) embedded in unconsolidated bioterrital sediments.
- Interval 4 (18.12–26.14 mbsf) represents basaltic lava and associated clinker produced on the top and leading edge of ‘a’ lava flows, much of which is fresh and unaltered, although zones of fracturing and alteration occur.

2.1. Hole M0105A

From 0.00 to 0.31 mbsf in Hole M0105A (Figure F1), a short interval of dominantly loose rhodoliths (less than 1 cm in diameter) in a dark gray matrix of unconsolidated bioterrital components (bivalves, gastropods, and foraminifers) and volcanoclastic medium sand-sized sediment was recovered (Figure F2A).

After a gap in core recovery between 0.31 and 7.43 mbsf, 26 cm of disturbed algal boundstone was recovered. It consists of thick, heavily bored crustose coralline algae (CCA) crusts with intergrown laminar corals, vermetids, and *Homotrema* (Figure F2B). Some dark medium sand-sized volcanoclastic grains are trapped in the CCA.

A second gap in core recovery extends from 7.69 to 12.95 mbsf. From this depth to 15.46 mbsf, coring disturbance from drilling is high and core recovery is low. The recovered material consists of disturbed and undisturbed coralg al boundstones with columnar and robust branching *Porites*, a

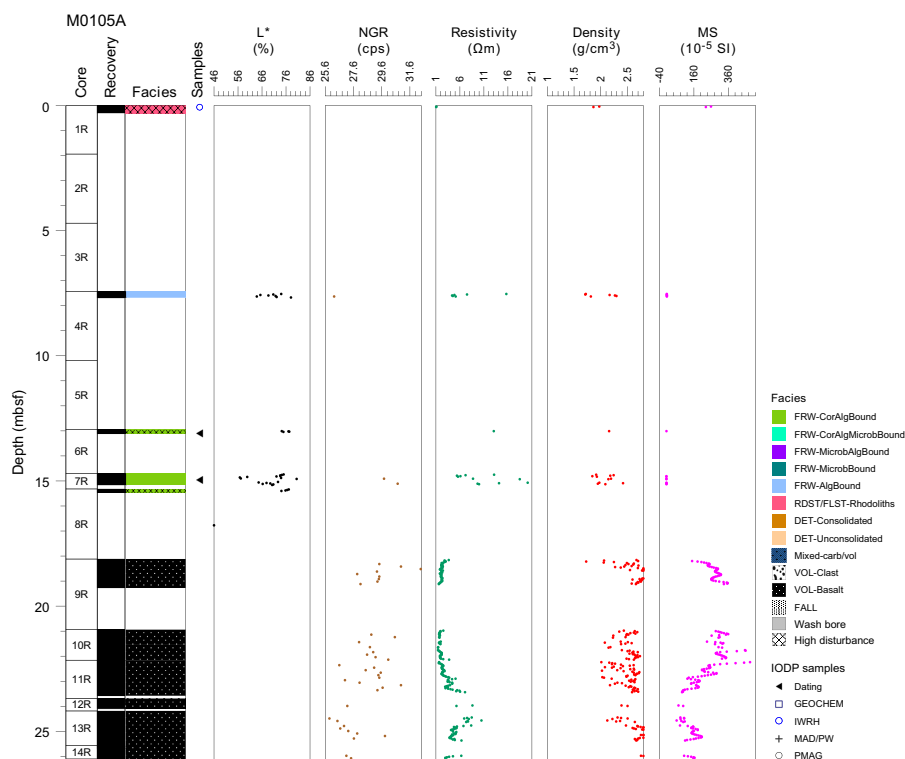


Figure F1. Lithostratigraphy and MSCL data, Hole M0105A. cps = counts per second, MS = magnetic susceptibility.

few *Cyphastrea*, and thin (less than 2 mm) bored CCA crusts (Figure F3). These fragments are embedded in an unconsolidated biodetrital matrix consisting of fragmented bivalves, gastropods, CCA, corals, and echinoid spines.

After a third gap in core recovery from 15.46 to 18.12 mbsf, the lithology changes to volcanic material. The contact between carbonate and lava was not recovered. From 18.12 mbsf to the bottom of the hole at 26.14 mbsf, the recovered material is primarily black, porphyritic (abundant olivine and pyroxene crystals), vesicular lava with a phaneritic groundmass texture (Figure F4A). Vesicles are generally abundant (10%–20%) and variable in size and character; in some areas they are millimeters in size (1–2 mm) and spherical (e.g., 25.36–25.98 mbsf), and in others they are larger (3–7 mm) and in many cases coalesced, for example at 21.00 mbsf. Locally, vesicles are filled with acicular aragonite. Lava characteristics vary locally. From 18.12 to 20.84 mbsf (Sections 389-M0105A-9R-1 and 10R-1), the lava is a coherent, unfractured, slightly altered lava rock with flow texture. From 20.84 to 23.58 mbsf (Section 11R-1), lava is still predominantly a coherent lava flow rock but is also locally fractured, with an orange-red staining along cracks. Some cracks and fractures are infilled with a reddish mud (Figure F4B). From 25.36 to 25.98 mbsf, the lava is variably altered, with a dark reddish color. It is fragmented with subrounded to subangular centimeter-sized fragments lacking a fine-grained component, possibly as lava clinker from an ‘a’a lava flow (Figure F4C).

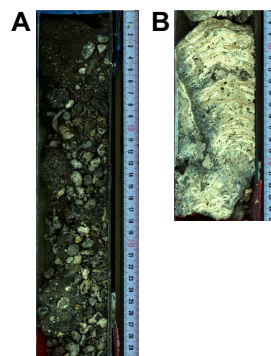


Figure F2. Lithologies, Hole M0105A. A. Rhodoliths in a dark gray unconsolidated biodetrital and volcanoclastic sandy matrix (1R-1, 0–30 cm). B. Heavily bored algal crust with intergrown encrusting or foliaceous corals vermetids and *Homotrema* (5R-1, 7–25 cm).

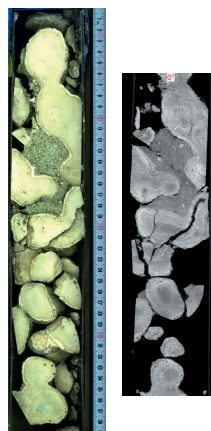


Figure F3. Lithologies, Hole M0105A. Fragmented columnar and robust branching *Porites* with thin, bored CCA crusts embedded in an unconsolidated biodetrital matrix (7R-1, 0–39 cm). Left: high-resolution linescan image. Right: X-ray computed tomography scan image (orthogonal view 0°–180°).

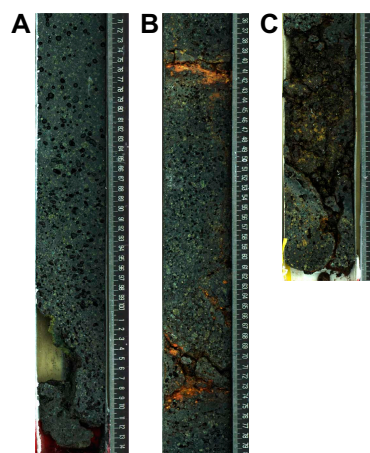


Figure F4. Lithologies, Hole M0105A. A. Black, porphyritic (abundant olivine and pyroxene crystals) vesicular lava with zones of centimeter-sized coalesced vesicles and zones of millimeter-sized round vesicles and a phaneritic groundmass texture (9R-1, 70–115 cm). B. Fractured porphyritic and vesicular lava with localized Fe-oxide-rich orange-red staining along cracks and reddish sediment fracture infills (11R-1, 35–80 cm). C. Dark reddish, altered, fragmental, vesicular lava deposit (13R-1, 120–147 cm).

3. Physical properties

Physical properties data for Site M0105 are shown in Table T2 in the Site M0096 chapter (Webster et al., 2025b).

3.1. Hole M0105A

A total of 7.49 m of core from Hole M0105A was scanned with the multisensor core logger (MSCL), and because the core exhibited moderate drilling-induced disturbance, 63% of the acquired data passed QA/QC (see Table T10 in the Expedition 389 methods chapter [Webster et al., 2025a]). A total of six discrete samples were taken for *P*-wave velocity and moisture and density (MAD) measurements. Digital linescans, color reflectance, and hyperspectral imaging were acquired on all cores.

3.1.1. Density and porosity

Data for density and porosity measurements are presented in Figures F1 and F5. MSCL density measurements range 1.71–3.03 g/cm³. The nature of the core quality (low recovery and drilling disturbance) means that the data quality is not optimal (see **Physical properties** in the Expedition 389 methods chapter [Webster et al., 2025a]). A total of six discrete samples were analyzed for MAD, giving a bulk density range of 2.12–2.84 g/cm³. Porosity values for the same samples range 14.2%–40.4%, and grain density values range 2.770–3.192 g/cm³.

3.1.2. *P*-wave velocity

P-wave velocity MSCL measurement yielded no data. A total of six samples were measured using the discrete *P*-wave logger. Dry measurement values range 3257–4626 m/s (Figure F6). *P*-wave velocity recorded for the samples after resaturation range 3898–5159 m/s. Because of the small number of *P*-wave data points, there are no apparent downhole trends.

3.1.3. Thermal conductivity

Thermal conductivity was measured on two cores (see Table T11 in the Expedition 389 methods chapter [Webster et al., 2025a]) and gave values of 1.957 and 2.187 (W/m·K).

3.1.4. Magnetic susceptibility

MSCL magnetic susceptibility data range -0.41×10^{-5} to 487.32×10^{-5} SI (Figure F1). Most of the magnetic susceptibility values fall between 100×10^{-5} and 487×10^{-5} SI and are associated with

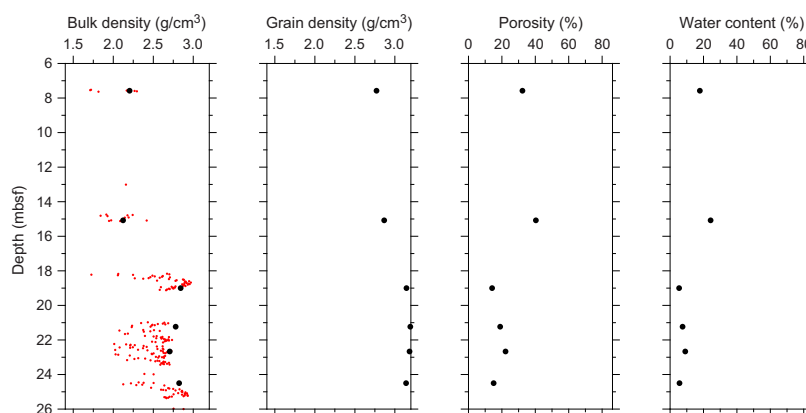


Figure F5. Physical properties, Hole M0105A. Black = discrete samples, red = MSCL.

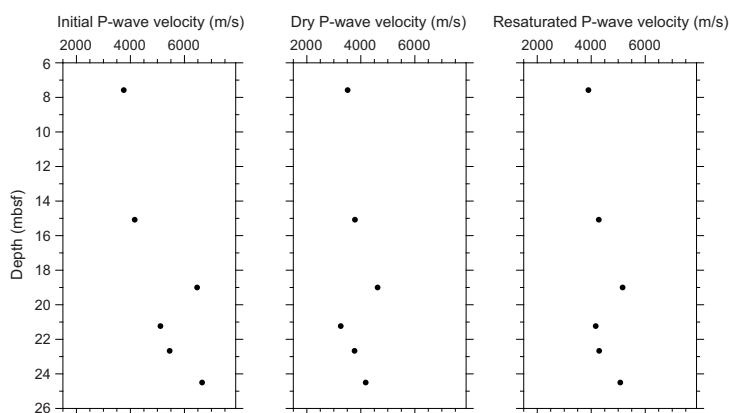


Figure F6. Initial, dry, and resaturated *P*-wave velocities measured on discrete samples, Hole M0105A.

lava (18–26 mbsf). At about 23 mbsf, magnetic susceptibility values decrease sharply from 487×10^{-5} to 70×10^{-5} SI.

3.1.5. Electrical resistivity

MSCL noncontact resistivity measurements yielded data ranging 1.05–20.12 Ωm , with most values ranging 2–10 Ωm (Figure F1). There are no apparent downhole trends.

3.1.6. Natural gamma radiation

MSCL natural gamma radiation (NGR) measurements range 26–32 counts/s (Figure F1), showing no apparent downhole changes.

3.1.7. Digital linescans, color reflectance, and hyperspectral imaging

All cores were digitally scanned, measured for color reflectance (where appropriate), and imaged with the hyperspectral scanner (see HYPERSPECTRAL in Supplementary material). Color reflectance L^* values vary between 0.09% and 80.42% (Figure F1), a^* varies between -1.94 and 6.91 , b^* varies between -0.83 and 19.69 , and a^*/b^* varies between -1.78 and 7.94 . Lower values in color reflectance below 18 mbsf reflect the change in lithology to lava (see Lithostratigraphy).

4. Geochemistry

4.1. Interstitial water

Two interstitial water samples were collected from Hole M0105A. These samples are generally within the range of other Expedition 389 interstitial water samples (see Tables T15 and T17 in the

Expedition 389 methods chapter [Webster et al., 2025a]). However, there are slight differences between the samples in their Al and Mn concentrations. Sample 1R-1, 1 cm (0.01 mbsf), has an Al concentration below detection limits (similar to most Expedition 389 interstitial water samples) and a Mn concentration of 0.13 mg/L, whereas Sample 1R-1, 3 cm (0.03 mbsf), has an Al concentration of 0.213 mg/L and a Mn concentration below detection limits.

4.2. Surface seawater

One surface seawater sample was collected at Site M0105 using a Niskin bottle deployed from the side of the vessel (see Figure F22 in the Expedition 389 methods chapter [Webster et al., 2025a]). The salinity, pH, alkalinity, and concentrations of ammonium were analyzed off shore, and major cations and anions were measured during the Onshore Science Party. The salinity, pH, alkalinity, ammonium, and major element chemistry measured for this sample are consistent with the other surface seawater samples taken during Expedition 389 and align with the expected values for conservative elements in seawater (see Tables T15 and T17 in the Expedition 389 methods chapter [Webster et al., 2025a]).

4.3. Bulk sediment

Two bulk sediment samples were taken from Hole M0105A (Figure F1) and analyzed for mineralogy, elemental composition, and carbon content. One sample was taken from algal boundstone at 7.46 mbsf (see Figure F10 in the Expedition 389 methods chapter [Webster et al., 2025a]) and the other sample from a lava unit at 22.96 mbsf.

4.4. Mineralogy

The basalt sample from Hole M0105A (11R-1, 80–84 cm; 22.96 mbsf) is composed of entirely plagioclase (46%) and pyroxene (54%), whereas the algal boundstone sample (4R-1, 3–9 cm; 7.46 mbsf) contains high-Mg calcite (23%), aragonite (66%), amphiboles (5%), Mn-carbonates (3%), and pyroxene (3%) (Table T2).

4.5. Elemental abundances

The elemental compositions of the two samples from Hole M0105A vary due to their differing lithologies (Table T3). The basalt sample (11R-1, 80–84 cm; 22.96 mbsf) contains 55,448 mg/kg Ca, 63,678 mg/kg Mg, 1,101 mg/kg Mn, 301 mg/kg Sr, 54,557 mg/kg Al, 76,838 mg/kg Fe, and 173,621 mg/kg Si. The algal boundstone sample (4R-1, 3–9 cm; 7.46 mbsf) contains 354,429 mg/kg Ca, 22,748 mg/kg Mg, 5,566 mg/kg Sr, and 1,428 mg/kg Fe and Al, Mn, and Si are below detection limits. Other elements (Ba, Br, K, P, S, Ti, Zr, Cr, Cu, Ni, Rb, V, and Zn) are minor constituents and/or below detection in the samples.

4.6. Carbon content

The basalt sample from Hole M0105A (11R-1, 80–84 cm; 22.96 mbsf) contains 0.70% total carbon (TC), 0.11% total organic carbon (TOC), and 0.59% total inorganic carbon (TIC). The algal boundstone sample (4R-1, 3–9 cm; 7.46 mbsf) contains 11.20% TC, 0.28% TOC, and 10.92% TIC (Table T4), calculating to approximately 90% CaCO₃, consistent with the sample's lithology, mineralogy, and element abundances.

Table T2. HighScore X-ray diffraction (XRD) mineral abundances, Site M0105. [Download table in CSV format.](#)

Table T3. Solid-phase elemental abundances, Site M0105. [Download table in CSV format.](#)

Table T4. TOC, TIC, and TC, Site M0105. [Download table in CSV format.](#)

5. Paleomagnetism

Seven plug samples were obtained from Hole M0105A. Low-field and mass-specific magnetic susceptibility (χ) measurements were carried out on all samples. Natural remanent magnetization (NRM) was measured for all samples, as well as remanence following stepwise alternating field (AF) demagnetization up to a peak AF of 20 mT for carbonate samples and 100 mT for lava samples. For further details, see [Paleomagnetism](#) in the Expedition 389 methods chapter (Webster et al., 2025a).

5.1. Hole M0105A

Two carbonate and five lava samples were obtained from Hole M0105A. The carbonate samples from 7.60 mbsf (Sample 4R-1, 15–18 cm) and 15.14 mbsf (Sample 7R-1, 42–44 cm) have low χ values of 4.04×10^{-8} and $-0.44 \times 10^{-8} \text{ m}^3/\text{kg}$, respectively. The lava samples have relatively high positive χ values throughout, ranging 4.07×10^{-6} to $0.16 \times 10^{-6} \text{ m}^3/\text{kg}$ with an arithmetic mean of $9.63 \times 10^{-6} \text{ m}^3/\text{kg}$. The initial NRM intensities of the carbonate samples are 1.07×10^{-3} and $0.30 \times 10^{-3} \text{ A/m}$, respectively. The initial NRM intensity of basaltic lava ranges 4.02 to 10.6 A/m with an arithmetic mean of 5.48 A/m. Values of χ and initial NRM co-vary, suggesting that concentration and properties of magnetic particles are the main drivers behind these variations (Figure F7).

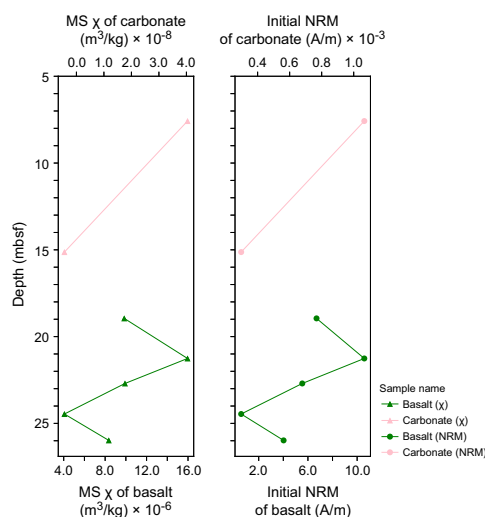


Figure F7. Magnetic susceptibility (MS) and NRM, Hole M0105A.

6. Geochronology

There are two U-Th dates from Site M0105, both from Hole M0105A, and they are dated to ~132 ky BP (see Tables T21 and T22 in the Expedition 389 methods chapter [Webster et al., 2025a]). Neither date is rejected based on the U-Th geochemistry. These data are consistent with the previously inferred timing of formation of the H2 terrace (Webster et al., 2009; Puga-Bernabéu et al., 2016).

References

- Puga-Bernabéu, Á., Webster, J.M., Braga, J.C., Clague, D.A., Dutton, A., Eggins, S., Fallon, S., Jacobsen, G., Paduan, J.B., and Potts, D.C., 2016. Morphology and evolution of drowned carbonate terraces during the last two interglacial cycles, off Hilo, NE Hawaii. *Marine Geology*, 371:57–81. <https://doi.org/10.1016/j.margeo.2015.10.016>
- Webster, J.M., Braga, J.C., Clague, D.A., Gallup, C., Hein, J.R., Potts, D.C., Renema, W., Riding, R., Riker-Coleman, K., Silver, E., and Wallace, L.M., 2009. Coral reef evolution on rapidly subsiding margins. *Global and Planetary Change*, 66(1–2):129–148. <https://doi.org/10.1016/j.gloplacha.2008.07.010>
- Webster, J.M., Ravelo, A.C., Grant, H.L.J., Rydzy, M., Stewart, M., Allison, N., Asami, R., Boston, B., Braga, J.C., Brenner, L., Chen, X., Chutcharavan, P., Dutton, A., Felis, T., Fukuyo, N., Gischler, E., Greve, S., Hagen, A., Hamon, Y., Hathorne, E., Humblet, M., Jorry, S., Khanna, P., Le Ber, E., McGregor, H., Mortlock, R., Nohl, T., Potts, D., Prohaska, A., Prouty, N., Renema, W., Rubin, K.H., Westphal, H., and Yokoyama, Y., 2025a. Expedition 389 methods. In Webster, J.M., Ravelo, A.C., Grant, H.L.J., and the Expedition 389 Scientists, Hawaiian Drowned Reefs. Proceedings of the International Ocean Discovery Program, 389: College Station, TX (International Ocean Discovery Program). <https://doi.org/10.14379/iodp.proc.389supp.2025>
- Webster, J.M., Ravelo, A.C., Grant, H.L.J., Rydzy, M., Stewart, M., Allison, N., Asami, R., Boston, B., Braga, J.C., Brenner, L., Chen, X., Chutcharavan, P., Dutton, A., Felis, T., Fukuyo, N., Gischler, E., Greve, S., Hagen, A., Hamon, Y., Hathorne, E., Humblet, M., Jorry, S., Khanna, P., Le Ber, E., McGregor, H., Mortlock, R., Nohl, T., Potts, D., Prohaska, A., Prouty, N., Renema, W., Rubin, K.H., Westphal, H., and Yokoyama, Y., 2025b. Site M0096. In Webster, J.M., Ravelo, A.C., Grant, H.L.J., and the Expedition 389 Scientists, Hawaiian Drowned Reefs. Proceedings of the International Ocean Discovery Program, 389: College Station, TX (International Ocean Discovery Program). <https://doi.org/10.14379/iodp.proc.389.102.2025>